Biol. Cybern. 84, 331–348 (2001)

Biological Cybernetics

A connectionist central pattern generator for the aquatic and terrestrial gaits of a simulated salamander

Auke Jan Ijspeert

Brain Simulation Laboratory & Computational Learning and Motor Control Laboratory, Hedco Neuroscience Building, Watt Way 3641, University of Southern California, Los Angeles, CA 90089, USA

Received: 5 April 2000 / Accepted in revised form: 11 September 2000

Abstract. This article investigates the neural mechanisms underlying salamander locomotion, and develops a biologically plausible connectionist model of a central pattern generator capable of producing the typical aquatic and terrestrial gaits of the salamander. It investigates, in particular, what type of neural circuitry can produce and modulate the two locomotor programs identified within the salamander's spinal cord; namely, a traveling wave of neural activity for swimming and a standing wave for trotting. A two-dimensional biomechanical simulation of the salamander's body is developed whose muscle contraction is determined by the locomotion controller simulated as a leaky-integrator neural network. While the connectivity of the neural circuitry underlying locomotion in the salamander has not been decoded for the moment, this article presents the design of a neural circuit that has a general organization corresponding to that hypothesized by neurobiologists. In particular, the locomotion controller is based on a body central pattern generator (CPG) corresponding to a lamprey-like swimming controller, and is extended with a limb CPG for controlling the salamander's limbs. The complete controller is developed in three stages: first the development of segmental oscillators, second the development of intersegmental coupling for the making of a lamprey-like swimming CPG, and finally the development of the limb CPG and its coupling to the body CPG. A genetic algorithm is used to determine the parameters of the neural circuit for the different stages, given a high-level description of the desired state space trajectories of the different subnetworks. A controller is thus developed that can produce neural activities and locomotion gaits very similar to those observed in the real salamander. By varying the tonic (i.e. non-oscillating) excitation applied to the network, the speed, direction and type of gait can be varied.

Correspondence to: A. J. Ijspeert
(e-mail: ijspeert@usc.edu)

1 Introduction

Locomotion is a fundamental skill for animals, that is needed for a variety of actions such as finding food, finding a mate for reproduction, escaping predators, and moving to a more friendly environment. The neural mechanisms underlying locomotion have therefore been extensively studied by neurobiologists, and in recent years there has been an increase in the use of computer simulations for testing and investigating models of locomotor circuits based on neurobiological observations. Examples of this include models of swimming in Tritonia (Getting 1989), bending reflex and crawling in leech (Lockery and Sejnowski 1993a; Cacciatore et al. 2000), swimming in lamprey (Ekeberg et al. 1991; Grillner et al. 1991; Hellgren et al. 1992; Wallén et al. 1992), swimming in Xenopus embryo (Roberts and Tunstall 1990), and locomotor circuits of chicks (O'Donovan et al. 1998).

Computer simulations can bring a useful contribution to neurobiology by investigating whether a potential model of the structure and function of a neural circuit can reproduce observations from physiological and ethological measurements. In the case of the control of locomotion, simulations are particularly useful for investigating the dynamical properties of the circuit. Furthermore, a computational approach has – by essence – several positive aspects: experiments are reproducible, all parameters of the model are controlled, neural activities can be accurately measured at all levels and simultaneously in all places, and the effect on behavior of altering parameters can be readily investigated (e.g., lesion studies on the real animal can be reproduced).

It is becoming more and more accepted that, in addition to neural mechanisms, the mechanical properties of the body play a primary role in the dynamics of locomotion. Indeed, body has its own dynamics and intrinsic frequencies with complex nonlinear properties, to which the frequencies, phases and shapes of motoneuron signals must be adapted for efficient locomotion and motor control. Furthermore, proprioceptive sensory feedback plays an important role in the shaping and

coordination of the neural activity with the mechanical activity. Several researchers have therefore coupled neuronal circuits to mechanical models of the body, and investigated the resulting dynamics, either in simulation (e.g., models of lamprey (Ekeberg 1993; Ekeberg et al. 1995; Ijspeert et al. 1999), of bipedal walking (Taga et al. 1991)) or by implementing the simulated neural circuits in robots (Beer et al. 1992; Cruse et al. 1995; Kimura et al. 1999).

In this article we take a similar approach, by simulating both the body and the locomotor circuit of the salamander. In particular, we are interested in the transition from aquatic to terrestrial locomotion, which has been an important step in vertebrate evolution. Studying the locomotor circuitry underlying the locomotion of the salamander – an animal that presents both types of locomotion – may therefore give some insight into the changes of the locomotor circuits that have accompanied this transition.

The salamander makes axial movements during locomotion. It swims using an anguiliform swimming gait, in which a rostrocaudal wave with a constant wavelength is propagated along the body (Frolich and Biewener 1992; Delvolvé et al. 1997). On ground, the salamander switches to a trotting gait, with the body making an S-shaped standing wave coordinated with the movements of the limbs. Opposite limbs are then out-of-phase, while diagonal limbs are in-phase. Note that, unlike supported quadruped trotting gaits, the salamander's trunk and tail usually remain in contact with the ground during the whole cycle. EMG recordings have shown that two different motor programs underly these typical gaits, with a traveling wave of neural activity for swimming and a mainly standing wave during trotting (Frolich and Biewener 1992; Delvolvé et al. 1997).

The locomotor circuitry responsible for these two motor programs has not been decoded for the moment. However, it has been hypothesized that the salamander's locomotor circuitry is based on a lamprey-like organization, with a lamprey-like CPG for the body segments extended by a limb CPG for controlling the limbs (Cohen 1988; Delvolvé et al. 1997). In this article, a computational model of a CPG based on such an assumption is developed. This work was strongly inspired by Ekeberg's neuronal and mechanical model of the lamprey (Ekeberg 1993). A simple two-dimensional mechanical simulation of a salamander in interaction with water or the ground is developed by extending Ekeberg's mechanical model of the lamprey. The muscular activity of the body is determined by a locomotor circuitry simulated as a leaky-integrator neural network. The locomotor circuitry is composed of a body CPG and a limb CPG. The body CPG is lamprey-like with an interconnection of 40 segmental networks for the generation of traveling waves of neural activity. The limb CPG comprises two interconnected oscillators projecting to the limb motoneurons and to the body CPG segments, creating a unilateral coupling between the two CPGs. While the general organization of the controller is set by hand, the time constants, biases and synaptic weights of the neurons are determined using a genetic algorithm. In previous work we successfully used the same approach to generate synaptic weights for a connectionist model of the lamprey's swimming CPG similar to Ekeberg's (Ijspeert et al. 1999). The development is here done in three stages: first the evolution of segmental oscillators, second the evolution of intersegmental coupling for the body CPG, and finally the evolution of the limb CPG connectivity. A neural circuit is developed that produces either a traveling wave or a standing wave of neural activity depending on the tonic input. The circuit can successfully control the speed, direction and type of gait of the simulated salamander.

In Sect. 2 we present the biomechanical simulation, and the general organization of the locomotor circuit in Sect. 3. In Sect. 4 we present the three stages of the development of the neural circuit with intermediate results for each stage.

2 Mechanical simulation of the salamander

The two-dimensional mechanical simulation of the salamander is an extension of Ekeberg's simulation of the lamprey (Ekeberg 1993). The 25-cm long body is made of ten rigid links representing the trunk and the tail, and four links representing the limbs (Fig. 1). The links are connected by one-degree-of-freedom joints, and the torques on each joint are determined by pairs of antagonist muscles simulated as springs and dampers. The signals sent by the motoneurons contract the muscles by increasing their spring constants. This

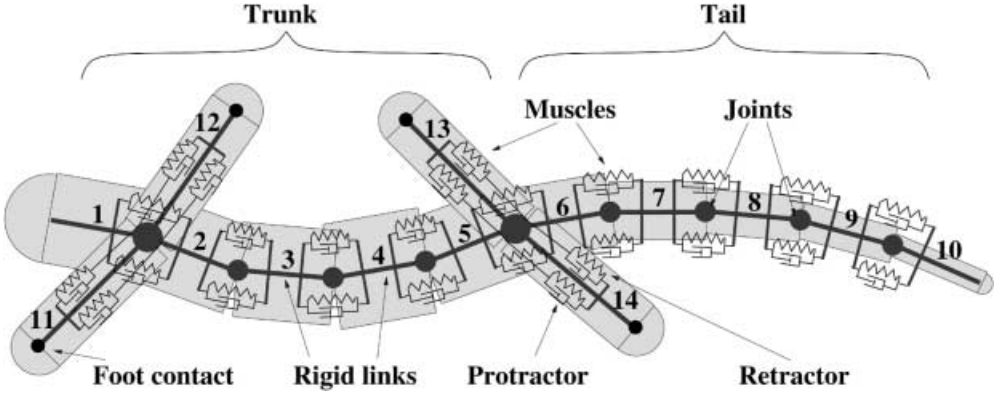

Fig. 1. Mechanical model of the salamander's body. The two-dimensional body is made of 14 rigid links connected by one-degree-of-freedom joints. Each joint is actuated by a pair of antagonist muscles simulated as spring and dampers. See text and Appendix A for details

biomechanical simulation is only a first approximation to a real salamander, and does not attempt to reproduce in detail the biomechanical properties of any specific salamander species.

The accelerations of the links are due to four types of forces: the torques due to the muscles, inner forces associated with the mechanical constraints due to the joints, contact forces between body and limbs, and the forces due to the environment. The forces due to the environment depend on whether the salamander is in water or on the ground. In water, it is assumed that each link (limb included) is subjected to inertial forces due to the water, with the forces being proportional to the square of the speed of the links relative to the water. On ground, all body links are subjected to a friction force, representing the trunk and the tail of the salamander as they slide on the ground when the salamander is trotting. As only the accelerations in the horizontal plane are calculated, we represent the contact of a limb with the ground as a friction force applied to the extremity of the limb link. We assume that the contact itself is determined by the signals sent to the horizontal protractor and retractor muscles. The limb is assumed to be in the air (i.e., without friction) when the signal of the protractor is larger than that of the retractor, and on the ground otherwise. The motoneurons for the retractor and protractor therefore not only determine the torque of the limb, but also its stand and swing phases. The mechanical simulation is described in more detail in Appendix A. The simulation is written in C language, and uses 4th-order Runge–Kutta integration for solving Newton's equations of motion (with 0.5-ms time steps).

3 Neuronal simulation of the CPG

The simulated neural controllers have a general organization that is predetermined by the experimenter, while their parameters – the synaptic weights, the neurons biases, and time constants – are determined by the genetic algorithm, given a description of the desired behavior of the controllers.

3.1 Hypothesized neural organization

The hypothesized organization of the salamander's locomotor circuit is shown in Fig. 2. The circuit is composed of a lamprey-like body CPG and a limb CPG made of two oscillators. The body CPG has a similar organization to the lamprey CPG with a chain of coupled segmental oscillators, and its motoneurons determine the muscular activity in the trunk and the tail. The chain is made of 40 segments as in most salamander species, rather than 100 as in the lamprey. The limb CPG controls the fore and hind limb motoneurons, and project unilaterally to the body CPG, with the anterior oscillator projecting to the trunk segments and the posterior oscillator projecting to the tail segments. In addition to connections coming from other neurons in the CPG, each neuron receives an input connection through which tonic (i.e., non-oscillating) drive is applied to the network (these connections can be seen as coming from reticulospinal neurons in the brainstem). As described below, the patterns of oscillations for swimming and trotting are modulated by that tonic input.

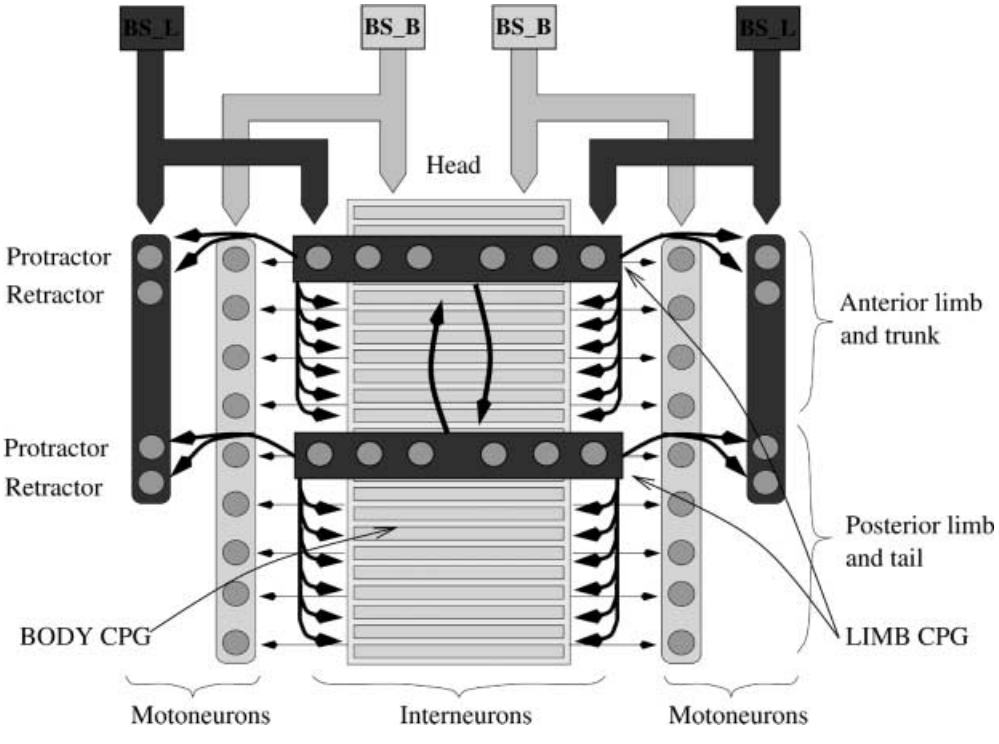

Fig. 2. Proposed organization of the salamander's locomotor circuitry. The circuitry is composed of a body CPG and a limb CPG. These CPGs can be activated by tonic input from the brainstem through four different pathways (left and right BS_B and BS_L for the body CPG and limb CPG, respectively)

3.2 Neuron model

In this work we develop connectionist models, i.e., models composed of neurons of intermediate complexity between abstract binary neurons used traditionally in artificial neural networks and detailed compartmental models used in computational neuroscience. Instead of simulating each activity spike of a real neuron, a neuron unit is modeled as a leaky integrator that computes the average firing frequency (Hopfield 1984). According to this model, the mean membrane potential m_i and the short-term average firing frequency x_i of a neuron i are governed by the following equations:

$$\tau_i \frac{\mathrm{d}m_i}{\mathrm{d}t} = -m_i + \sum_j w_{i,j} x_j \tag{1}$$

$$x_i = (1 + \mathrm{e}^{(m_i + b_i)})^{-1} \tag{2}$$

where b_i is the neuron's bias, τ_i is a time constant associated with the passive properties of the neuron's membrane, and $w_{i,j}$ is the synaptic weight of a connection from neuron j to neuron i. Each neuron exhibits an internal dynamics and even small networks of these neurons have proven able to produce rich dynamics (Beer 1995). Compared to the real neuronal circuit in the salamander, each of these neuron units should be considered to represent a population of functionally similar neurons. The neural simulation uses the same numerical integration procedure as the mechanical simulation, except that the time step is 10 ms.

4 Staged evolution of the CPG

The locomotion controllers are developed in three stages: first the development of segmental oscillators, second the development of intersegmental coupling in the body CPG, and finally, the development of the connectivity of the limb CPG. For the three stages, the same genetic algorithm is used for determining the parameters of a network whose architecture is defined by hand.

4.1 Genetic Algorithm

For parameter determination a genetic algorithm (Holland 1975; Goldberg 1989) is used with real number encoding instead of the traditional binary encoding. The parameters of a neural network are encoded (see next sections) into a chromosome, i.e., a fixed-length string of genes which are real numbers between 0.0 and 1.0. Each chromosome (i.e. each potential solution) is given a fitness value according to a fitness function that determines the desired behavior of the neural network (see next sections).

The algorithm starts with an initial population of N randomly created chromosomes. At each generation, a fixed number C of children chromosomes are generated using two operators: crossover and mutation. The crossover operator chooses couples of parents, with a rank-based probability for breeding (the jth fittest chromosome has a probability $P(j) = \frac{N-(j-1)}{1+2+\cdots+N}$ of being chosen). Couples of children are created from couples of parents either by two-point crossover (probability P_X) or by simply copying the two parents (probability $1 - P_X$). Two-point crossover consists of randomly choosing two locations in the string of genes and creating children by swapping substrings of the parent chromosomes.

The mutation operator mutates each gene of the children with a probability P_M and the mutation consists of adding or subtracting a small random number within a mutation range R:

$$new\_value = old\_value + R \cdot rand$$

where *rand* is a random number $\in [-0.5, 0.5]$. In the first stage, a pruning operator is also applied which randomly prunes a connection (probability P_P) by setting the gene to the value corresponding to a null weight. The children are then evaluated, and the size of the population is kept constant by rejecting – at each generation – the worst solutions of the increased population (old population plus children). The genetic algorithm parameters used for the three stages are given in Table 1.

Table 1. Parameters of the genetic algorithm

	N	C	P_X	P_M	R	P_P
Stage 1	100	30	0.5	0.4	0.2	0.1
Stage 2	100	30	0.5	0.4	0.2	0.0
Stage 3	50	16	0.5	0.4	0.2	0.0

4.2 First stage: segmental oscillators

In this first stage, segmental oscillators are developed by evolving the connectivity and the neuron parameters of a eight-neuron neural network.

4.2.1 Encoding and fitness function. A segmental network is encoded into a 39-gene chromosome. The network is assumed to have a left-right symmetry, with – on each side – one motoneuron and three types of interneurons. Neurons are either inhibitory or excitatory. For each type of interneuron, a chromosome encodes the time constant of the neuron, its bias, its sign, the synaptic weight of its input connection from the brainstem, and the synaptic weights of the outwards connections to itself and the other seven neurons (36 genes). A chromosome also encodes the motoneuron's time constant, and the bias and synaptic weight of the input connection (three genes). Similarly to the lamprey, motoneurons are assumed to be excitatory, and to not participate in the rhythmogenesis (i.e., they project only to the muscles and not to other neurons). The parameter values are linearly decoded from the genes ($\in [0.0, 1.0]$) with the following boundary values: 20.0 and 500.0 ms for the time constants, -10.0 and 10.0 for the biases, and 0.0 and 10.0 for the synaptic weights. The neuron is inhibitory when its sign gene is smaller than 0.5, and excitatory otherwise.

The fitness function is defined to reward solutions that oscillate regularly with left and right motoneurons out-of-phase, and whose frequency of oscillation can be varied with the level of tonic drive applied to the network. In particular, the frequency of oscillation – as well as the amplitude of the motoneuron's oscillation – should increase monotonically with the level of tonic drive. Mathematically, the fitness function is a product of four factors:

$$fit1 = fit\_oscil \cdot fit\_regularity \cdot fit\_oscil\_phase \cdot fit\_freq\_range$$

Each factor is a function that varies linearly between 0.05 and 1.0 when its corresponding variable varies between a bad and a good boundary (Table 2). The good boundaries therefore define the target specifications of the networks. The fact that the fitness function is a product rather than a sum ensures that solutions that perform equally in all four aspects rewarded by the factors will be more favored compared to controllers performing well in some aspects but not in others. In order to determine the range of frequencies at which the networks can oscillate, an evaluation consists of a set of neural simulations of fixed duration (12 s) with different levels of tonic drive.

4.2.2 Results. Ten runs starting with different initial random populations of 100 chromosomes were carried out for 600 generations. All runs except one converged to networks capable of producing regular oscillations whose frequencies could be modulated with the level of tonic drive applied to them.

Figure 3 and Table 3 give the parameters of the best evolved network – it is the segmental oscillator which will be used in the next stages. That network is made of motoneurons and three types of inhibitory interneurons. It can be considered as a half-center network made of two sub-networks which create oscillations through mutual inhibition. Burst termination, i.e., the switch of neural activity from one side to the other, is ensured by network (rather than neural) properties, namely delayed inhibition, including self-inhibition.

The level of tonic drive can be varied over a large range (from 0.0 to 2.3, in arbitrary units of brainstem activity) in which the frequency and the amplitude of oscillation increase monotonically with the input. A range of frequencies from 0.8 to 9.3 Hz can thus be covered. The oscillations produced (Fig. 4) are due to a unique and stable limit cycle in the state space of the network (we ran the simulations with a variety of random initial conditions, and the network always converged to the same oscillations). For this network, when the tonic input is increased above the limit of the monotonic range, the frequency of oscillation decreases until zero. For most of the produced segmental networks, however, the monotonic increase in frequency stops when excessive excitation leads to the limit cycle collapsing into a single attractor, depending on the initial conditions: i.e., neurons saturate and the network converges quickly to a stable left-right asymmetric state. Note that this segmental network oscillates even without tonic excitatory input because of the positive biases of

Table 2. Variables and boundaries for the fitness function of the first stage. θ_{oscil} is the phase between left and right motoneurons. It is measured as a ratio of the cycle duration (i.e., 0.5 means anti-phase). The frequency range is indirectly optimized by optimizing the ratio between maximum and minimum frequencies, with 0.8 Hz being the lowest measurable frequency (i.e., min_freq $\geq$ 0.8)

Function	Variable	Bound [*bad*, *good*]
fit_oscil	Number of extrema	[0, 20]
fit_regularity	SD of periods	[0.05, 0.0]
fit_oscil_phase	$\lvert\theta_{oscil} - 0.5\rvert$	[0.5, 0.0]
fit_freq_range	max_freq/min_freq	[1.0, 15.0]

Table 3. The best segmental oscillator. *M* stands for motoneuron and *A*, *B* and *C* are interneurons. The lower part of the table gives the synaptic weights from all connections from M_l, A_l, B_l and C_l on the left side (M_r, A_r, B_r and C_r stand for their corresponding neuron on the right side). The connections from the right, i.e., contralateral, side are symmetric. All neurons except interneurons *A* receive input from left and right pathways from the brainstem (BS_l and BS_r). See also Fig. 3

	M_l	A_l	B_l	C_l	BS_l
τ	20 ms	297 ms	57 ms	20 ms	–
b	0.2	2.9	−6.4	5.6	–
M_l	–	–	−8.2	−10.0	5.0
A_l	–	–	–	–	–
B_l	–	−2.1	−5.8	–	8.2
C_l	–	−2.2	−9.7	−4.0	2.9
M_r	–	–	–	−4.1	–
A_r	–	−4.4	−3.4	−2.8	–
B_r	–	–	−8.8	−9.6	–
C_r	–	–	–	−9.9	–

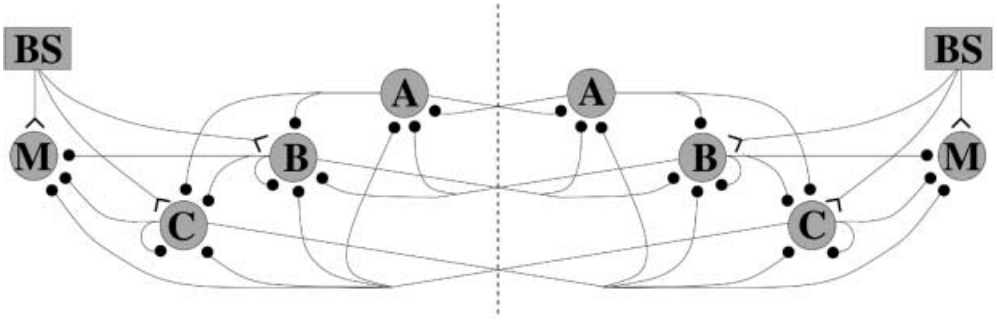

Fig. 3. Connectivity of the segmental oscillator. *A*, *B* and *C* are three types of interneurons, and *M* are the motoneurons. BS indicates the inputs from the brainstem

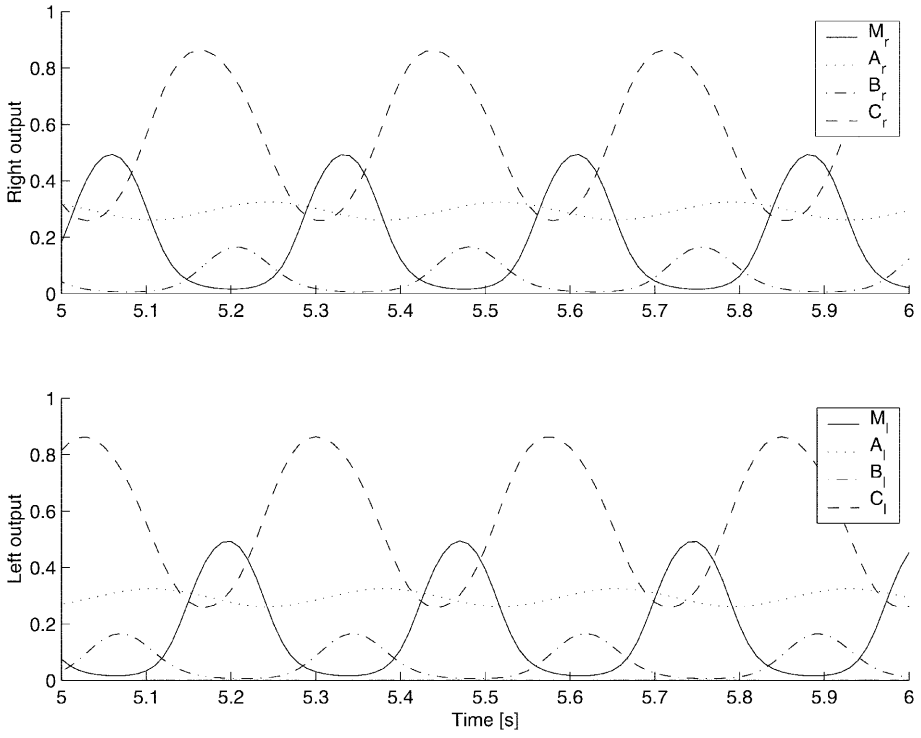

Fig. 4. Neural activity in the segmental oscillator. M_l, A_l, B_l and C_l correspond to the neurons on the left side of the oscillator, and M_r, A_r, B_r and C_r to those on the right side

neurons M, A and C (these neurons produce a non-zero output in the absence of an excitatory input).

4.3 Second stage: intersegmental coupling

The aim of this stage is to develop a complete body CPG made of 40 segments (similar to most salamander species) which can propagate a traveling rostro caudal wave for swimming. The best oscillator of the previous stage is chosen as a template segmental oscillator and copied 40 times. Note that having identical segmental oscillators along the spinal cord is only an approximation of the salamander's spinal circuitry, as there probably exist variations in the connectivity and density of neurons depending on the position of the segment. The coupling between segments is obtained using synaptic spreading similar to that used to model the lamprey's CPG (Williams 1992; Ekeberg 1993), in which a connection between two neurons in a segmental oscillator is projected to corresponding neurons in neighboring segments. In Williams (1992), the synaptic spreading is only to the nearest neighbor segment, while in Ekeberg (1993), it is up to ten segments of the 100-segment lamprey. In our model of the salamander CPG, projections are limited to five segments of the 40-segment body. This is an arbitrarily chosen limit (the lengths of intersegmental projections are currently not known in the salamander) which leads to relatively short-range intersegmental coupling. Note also that it is currently not known how exactly localized the rhythmogenesis is: for instance, whether all isolated single segments of the salamander's spinal cord can be made to oscillate independently as in the lamprey. Preliminary experiments reported in Delvolvé et al. (1999) showed that oscillations could be induced in small parts of two and three segments of the rostral half of the spinal cord. This supports the idea that rhythmogenesis is distributed, and that the body CPG can be considered as a chain of discrete coupled oscillators.

4.3.1 Encoding and fitness function. A chromosome encodes the extent of the projections of the segmental connections to corresponding neurons in neighboring segments in both the rostral and caudal directions. As the chosen template segmental oscillator has 28 connections (not including the connections from the brainstem), a chromosome has twice 14 genes for encoding the projections in both directions (a left-right symmetry is again assumed). The extent of the projection is measured in terms of the number of segments, and genes ($\in [0.0, 1.0]$) are transformed into integers between 0 and 5 (maximal projection). The connection weights of the segmental networks correspond to those of the template segmental oscillator, with a rescaling that depends on the extent of the intersegmental coupling: the weight of a connection to a neuron is divided by the number of segments it receives input from.

The fitness function is defined to reward body CPGs which: (1) produce regular oscillations in all 40 segments, (2) propagate a traveling wave from head to tail with a constant phase lag along the spinal cord, and (3) have their frequency of oscillation varied by the level of tonic drive. The target phase lag between consecutive segments is fixed to be 2.5% of the cycle duration, so that the 40-segment CPG produces one complete wave (i.e., a 100% phase lag between the first and last segment), as observed in real salamanders (Frolich and Biewener 1992; Delvolvé et al. 1997). The mathematical definition of the fitness function is:

$$fit2 = fit\_oscil \cdot fit\_regularity \cdot fit\_oscil\_phase \cdot fit\_spinal\_phase \cdot fit\_freq\_range$$

Similarly to the fitness function of the first stage, these factors vary between 0.05 and 1.0 when their corresponding variable varies between a bad and a good boundary (Table 4). In order to evaluate the range of frequencies over which the chain of oscillators can oscillate, solutions are evaluated by a set of 12-s long simulations with different levels of tonic input.

Table 4. Variables and boundaries for the fitness function of the second stage. θ_{oscil} is the phase between left and right motoneurons in segment 20. θ_{spinal} is the average phase between consecutive segments. Phases are measured as ratios of the cycle duration

Function	Variable	Bound [*bad*, *good*]
fit_oscil	Number of extrema	[0, 30]
fit_regularity	SD of periods	[0.05, 0.0]
fit_oscil_phase	$\lvert\theta_{oscil} - 0.5\rvert$	[0.5, 0.0]
fit_spinal_phase	$\lvert\theta_{spinal} - 0.025\rvert$	[0.5, 0.0]
fit_freq_range	max_freq/min_freq	[1.0, 15.0]

4.3.2 Results. Ten runs were carried out for 100 generations. All runs converged to intersegmental couplings that propagate a stable rostro caudal traveling wave with a wavelength corresponding approximately to the length of the spinal cord. Note that coupling neural oscillators can lead to unstable behavior even when the oscillators have the same intrinsic frequency (as is the case here). Within the initial random populations, for instance, a large majority of the random couplings led to very irregular oscillations.

Figure 5 illustrates the neural activity in the best evolved body CPG, and the resulting swimming gait when the motoneuron signals are used to drive the mechanical simulation. Note that as the mechanical simulation represents the body with only ten links, the signals from nine equally spaced segmental oscillators (from segment 4 to segment 36) are used to determine the muscular torques of the nine joints of the body (trunk and tail). Tonic signals are then also sent to the retractor muscles of the limbs in order to keep them against the body.

When tonic input is applied to all segments, the body CPG spontaneously propagates a rostrocaudal traveling wave. The phase lag between consecutive segments is

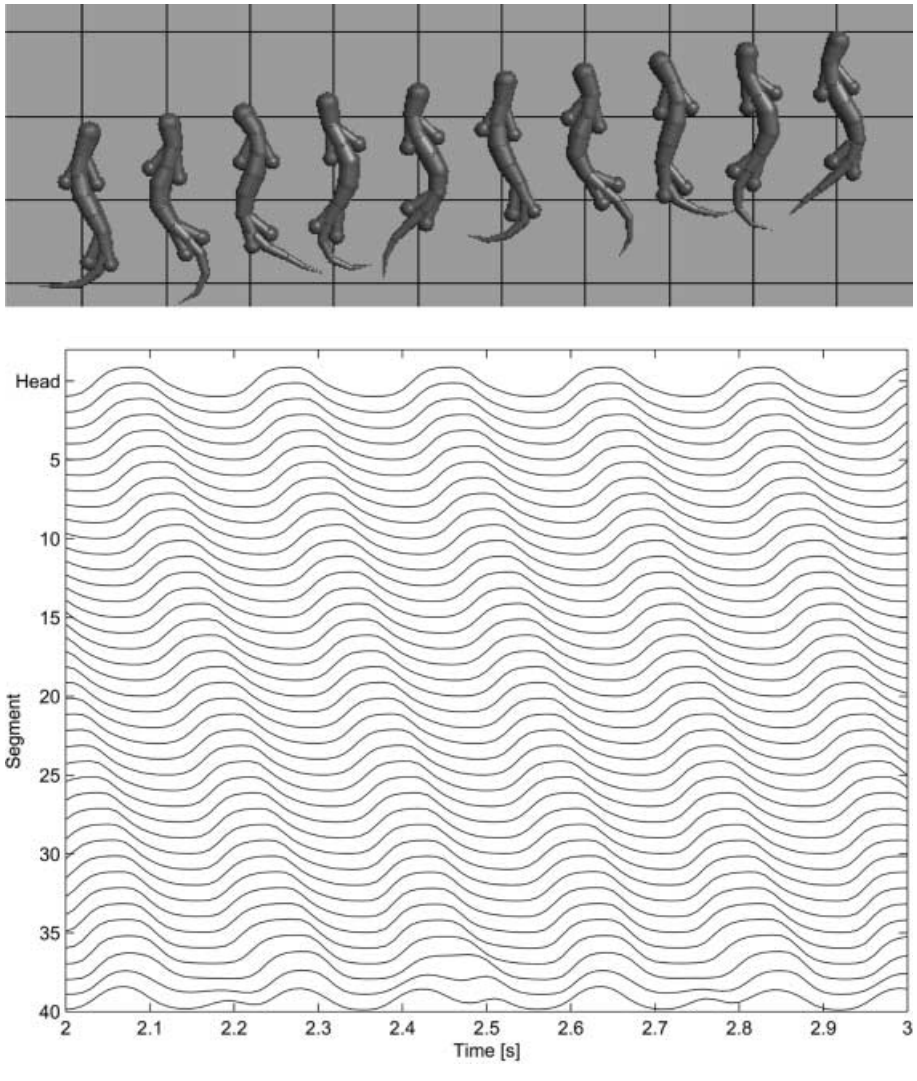

Fig. 5. Swimming. *Top:* mechanical simulation. *Bottom:* neural activity in the body CPG (for clarity, only the activity of the left motoneurons is shown)

constant over the spinal cord, except at the tail where the lag decreases slightly and where oscillations become less regular. The extents of the intersegmental coupling responsible for the lag are on average longer in the rostral direction (average of 2.6 segments) than in the caudal direction (average of 1.5 segments, see Table 5).

Similarly to the isolated segmental oscillators, the frequency of oscillation can be modulated by the tonic input, with the frequency of oscillation increasing with the input level. Increasing the frequency leads to an increase of the speed of swimming (Fig. 6). The range of frequencies of the body CPG is smaller than that of the isolated segmental oscillator. The best evolved body CPG covers a range of frequencies from 2.7 to 5.4 Hz (when the level of tonic input varies between 0.9 and 1.7). Inputs below 0.9 lead to unstable oscillations which have on average frequencies higher than just above 0.9, and the frequency of oscillation saturates for inputs above 1.7.

Table 5. Intersegmental coupling of the best body CPG. The rescaled synaptic weights of the segmental oscillators are given. Numbers in brackets indicate coupling extents in the rostral and caudal directions, respectively. Only connections from the left neurons are shown; the connections from the right side are symmetric. Input is given by the left-right pathways from the brainstem to the body CPG (BS_B_l and BS_B_r)

	A_l	B_l	C_l	BS_B_l
M_l	–	−1.2 [5, 1]	−5.0 [1, 0]	5.0
A_l	–	–	–	–
B_l	−0.3 [3, 4]	−1.2 [1, 3]	–	8.2
C_l	−0.3 [5, 2]	−1.6 [5, 0]	−0.7 [3, 2]	2.9
M_r	–	–	−1.3 [1, 1]	–
A_r	−1.5 [1, 1]	−1.1 [1, 1]	−0.7 [3, 0]	–
B_r	–	−1.3 [2, 4]	−1.4 [5, 1]	–
C_r	–	–	−5.0 [0, 1]	–

The phase lag between segments also varies with the level of tonic input, but less significantly than the frequency. The phase lag between consecutive segments remains approximately at 2.5% of the cycle duration, which corresponds to a phase of 100% between the head and the tail of the 40-segment body CPG. Such a property has also been observed in the lamprey, which keeps a constant wavelength while its frequency of oscillation can vary over a large range. Figure 6 (top) gives the minimum, maximum, and mean value of the phase between consecutive segments along the spinal cord. It can be seen that there is little difference between minimum and maximum values, which means that the phase lag does not vary appreciably along the spinal cord for any level of tonic input. Note that the phase lag can be modulated to some extent by varying the input given to the most rostral segments compared to the other segments. For instance, giving extra excitation to these segments leads to a larger phase lag between segments (and therefore a reduced wavelength) over the whole spinal cord (data not shown). We were not able to reduce or inverse the phase lag (for instance, by giving less excitation to the most rostral segments or more to the most caudal). The spontaneous phase lag induced by the intersegmental coupling appears therefore to correspond to the minimal lag between consecutive segments.

Similarly to Ekeberg's lamprey (Ekeberg 1993), turning during swimming can be induced by applying asymmetrical input between left and right sides of the spinal cord. The asymmetry of input leads to higher

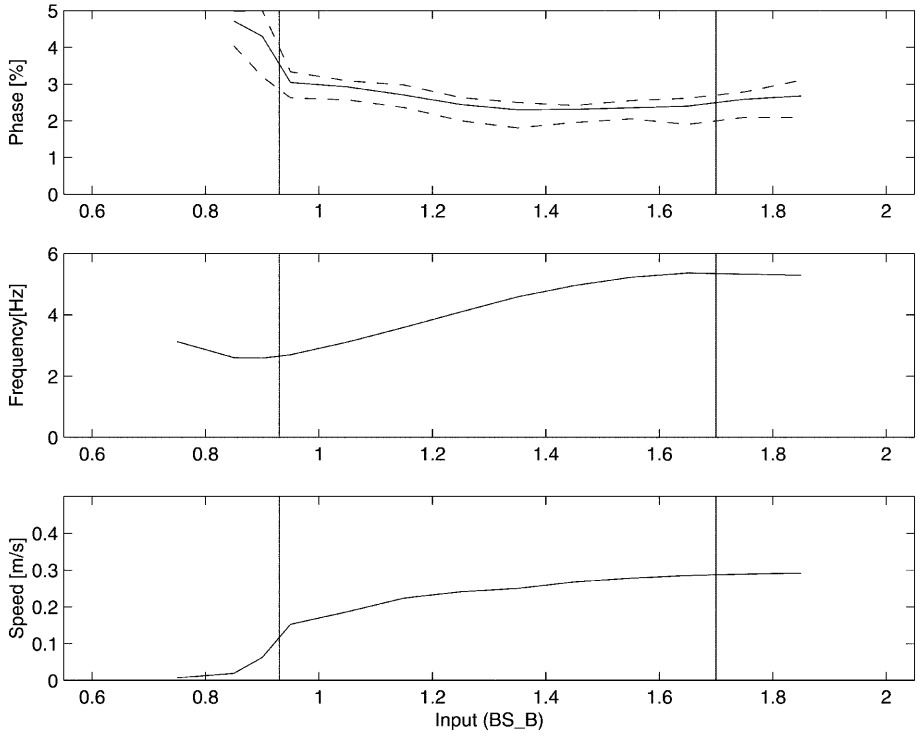

Fig. 6. Body CPG: influence of the tonic input on the phase lag along the spinal cord, the frequency of oscillation, and the speed of swimming. The vertical lines determine the region in which the frequency increases monotonically with the tonic input

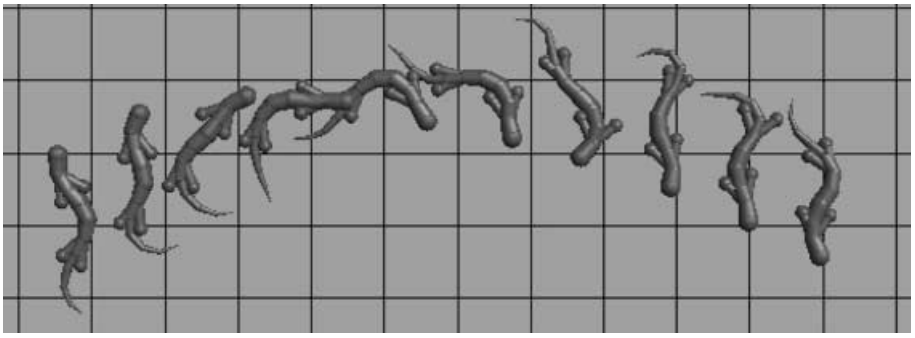

Fig. 7. Turning during swimming induced by asymmetric tonic input

amplitudes of motoneuron signals on the side receiving extra excitation, which leads therefore to larger contractions of the muscles on that side. When the asymmetry is of short duration, it changes the heading of swimming, and when it is long, the salamander swims on a circle (Fig. 7).

4.4 Third stage: coupling between the limb CPG and the body CPG

In this last stage, a complete locomotor circuit is obtained by adding a limb CPG to the body CPG. The limb CPG is made of two oscillators that are copies of the template segmental oscillator of the body CPG. The limb oscillators are mutually coupled, and project to the motoneurons of their respective limbs. They also project unilaterally to the interneurons of the segmental oscillators of the body CPG, with the anterior oscillator projecting to the trunk segments and the posterior oscillator projecting to the tail segments (see Fig. 2). The aim is to develop a locomotor circuit that produces the swimming gait when tonic input is applied to the body CPG, and the trotting gait when tonic input is applied to *both* the body and the limb CPGs.

4.4.1 Encoding and fitness function. A chromosome encodes the weights of the connections between the limb oscillators, from the oscillators to the limb motoneurons, and from the limb oscillators to the segmental oscillators of the body. It also encodes the parameters for the limb retractor and protractor motoneurons. A chromosome is 60 genes long. Left-right and anterior-posterior symmetries are imposed. Connections from the oscillators to the limb motoneurons can have weights between -10.0 and 10.0, while connections between limb oscillators and from the limb oscillators to the body oscillators can have weights between -2.0 and 2.0.

For this stage, the fitness function is based on both the neural and the mechanical simulations. Its aim is to generate controllers which are capable of producing the trotting gait, and controllers are therefore tested in conditions in which both the body and the limb CPGs receive tonic input. The fitness function is defined to reward locomotor circuits which: (1) produce limb motoneuron signals with non-zero amplitude, (2) have retractor and protractor motoneurons oscillating out-of-phase, (3) have anterior and posterior oscillators out-of-phase (to ensure a trotting gait), (4) can produce fast trotting gaits, and (5) can cover a large range of speeds when the level of input applied to both the body and the limb CPGs is varied. Note that the first two points are theoretically not necessary for generating trotting gaits, but were added to accelerate the convergence to interesting solutions. The evaluation of a locomotor circuit consists of a set of 6-s-long simulations with different levels of tonic inputs, in order to determine the range of speeds they can produce. Mathematically, the definition of the fitness function is:

$$\begin{aligned} fit3 = {} & fit\_ampl \cdot fit\_limb\_mn\_phase \\ & \cdot fit\_limb\_oscil\_phase \cdot fit\_max\_speed \\ & \cdot fit\_speed\_range \end{aligned}$$

These functions are similar those of the previous stages. Their variables and boundaries are given in Table 6.

Table 6. Variables and boundaries for the fitness function of the third stage. *mn_ampl* corresponds to the average amplitude of the limb motoneurons oscillations. θ_1 corresponds to the phase between limb retractor and protractor, and θ_2 to the phase between the anterior and posterior oscillators. *min_s* and *max_s* correspond respectively to the minimum and maximum trotting speeds

Function	Variable	Bound [*bad*, *good*]
fit_ampl	*mn_ampl*	[0.0, 0.5]
fit_limb_mn_phase	$\lvert\theta_1 - 0.5\rvert$	[0.5, 0.0]
fit_limb_oscil_phase	$\lvert\theta_2 - 0.5\rvert$	[0.5, 0.0]
fit_max_speed	*max_s* [m/s]	[0.0, 1.0]
fit_speed_range	$\frac{max\_s - min\_s}{max\_s}$	[1.0, 15.0]

4.4.2 Results. Ten evolutions were carried for 30 generations. Figure 8 shows the trotting gait produced by the best complete locomotor circuit, when tonic drive is applied to both the limb and the body CPGs. The trotting gait is due to the out-of-phase relation of the two limb oscillators. These oscillators activate the limbs' retractor and protractor motoneurons for the stepping movement. The unilateral coupling from the limb oscillators to the body segmental oscillators forces the body CPG to produce a standing wave instead of a traveling wave. During trotting, there is no phase lag between segments in the body (they oscillate in synchrony), except for the abrupt change of phase at the level of

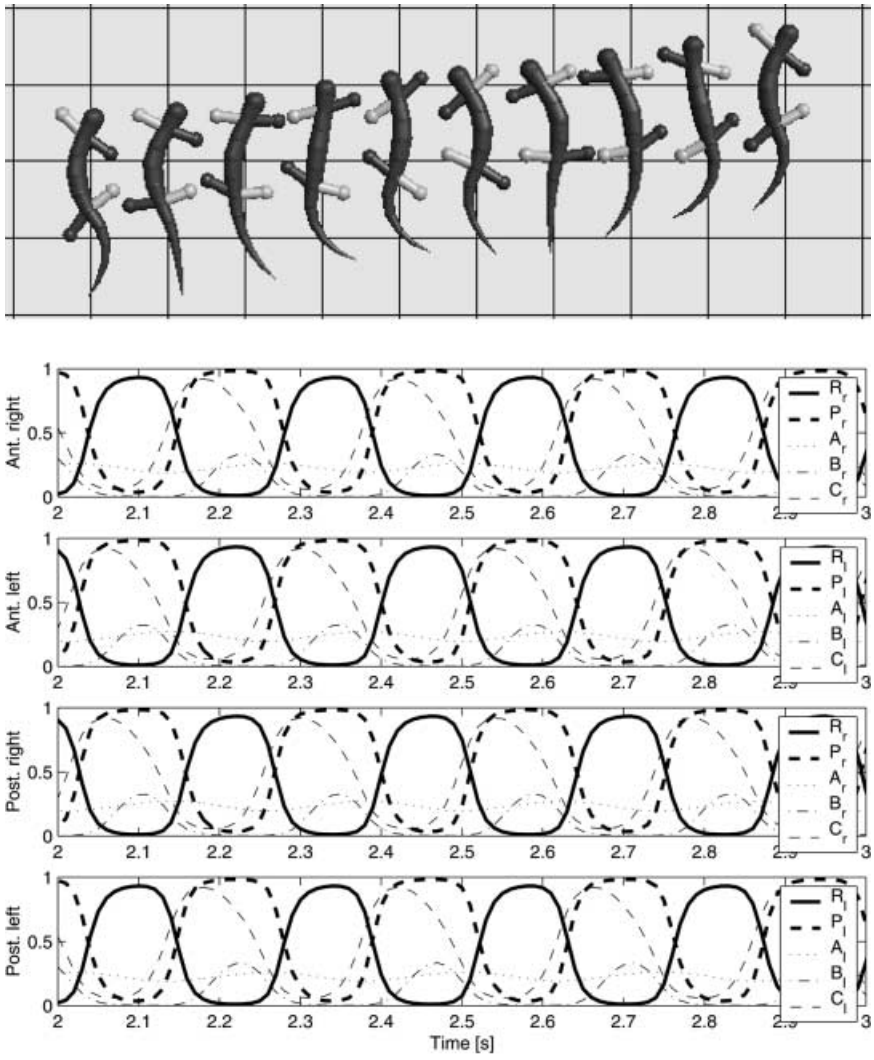

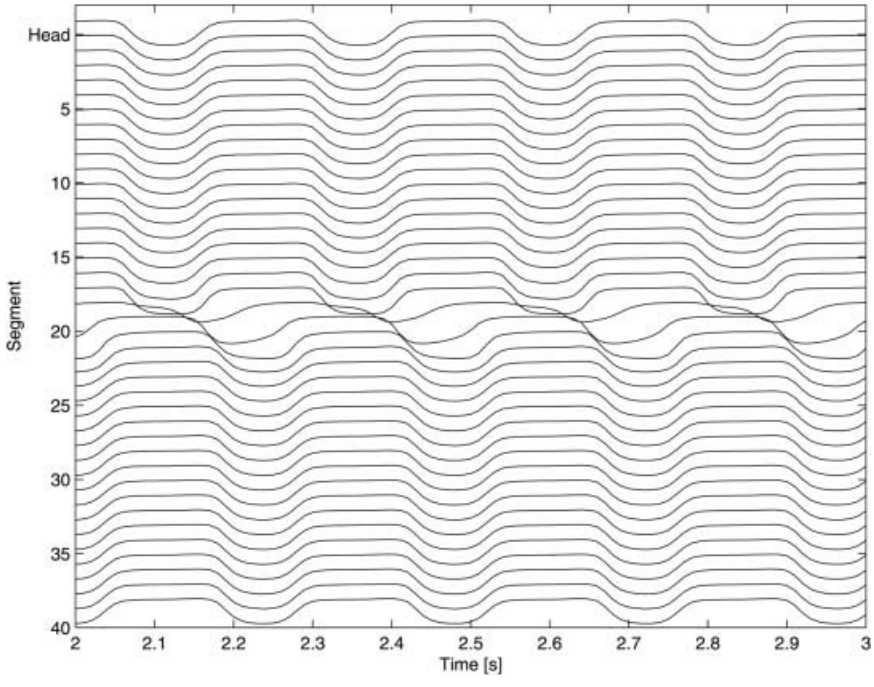

Fig. 8. Trotting. *Top:* mechanical simulation. Limbs in contact with the ground are drawn in white. *Middle:* neural activity in the limb CPG (both the anterior and the posterior oscillators). R_r and R_l indicate right and left retractor neurons, and P_r and P_l indicate right and left protractor neurons. *Bottom:* neural activity in the body CPG (left motoneurons)

the posterior girdles (segment 20), i.e., where the influence of the anterior limb oscillator ends and that of the posterior limb oscillator begins. The change of phase in that region leads the trunk and tail segments to oscillate out-of-phase, with the body therefore performing the typical S-shaped standing wave. This neural standing wave and, in particular, the synchrony of all segments of the trunk are very similar to EMG recordings during trotting in the real salamander (Frolich and Biewener 1992; Delvolvé et al. 1997). Note, however, that the neural activity in the tail has been observed to be more complex than the one simulated here, with two successive waves traveling in opposite directions (Delvolvé et al. 1997) instead of a single burst synchronous in all segments. Table 7 gives the connectivity of the limb CPG and its projections to the limb motoneurons and the body oscillators.

Table 7. Connectivity of the limb CPG. Only the connections from the neurons the left side of the anterior oscillator are given (connections from the right side and from the posterior oscillator are symmetrical). *R* and *P* stand for retractor and protractor motoneurons. pA_l and pA_r are left and right neurons *A* in the posterior oscillator. bA_l and bA_r are left and right neurons *A* in a body CPG oscillator (all oscillators in the trunk receive the same projections from the anterior oscillator, as do the tail oscillators from the posterior oscillator)

	A_l	B_l	C_l	BS_L_l
R_l	–	−8.2	−10.0	3.3
P_l	−1.4	–	−2.3	5.4
A_l	–	–	–	–
B_l	−2.1	−5.8	–	8.2
C_l	−2.2	−9.7	−4.0	2.9
R_r	–	−0.7	−2.7	–
P_r	−0.4	−7.4	−10.0	–
A_r	−4.4	−3.4	−2.8	–
B_r	–	−8.8	−9.6	–
C_r	–	–	−9.9	–
pA_l	−2.0	−1.5	−0.5	–
pB_l	−0.8	−0.3	−0.9	–
pC_l	–	−1.2	−1.9	–
pA_r	−1.0	−1.3	−0.6	–
pB_r	−1.6	−1.1	−0.1	–
pC_r	−1.2	−1.1	−0.7	–
bA_l	−0.3	−0.7	−1.9	–
bB_l	−0.9	−0.9	−1.2	–
bC_l	−0.4	−0.3	−0.2	–
bA_r	−0.9	–	−1.1	–
bB_r	−0.6	−1.7	−0.2	–
bC_r	−0.2	−0.1	−1.0	–

Interestingly, although the fitness function did not reward any particular body-limb coordination, rewarding the speed of trotting led to controllers that produced a body-limb coordination very similar to the real salamander (Fig. 8, top). The body is indeed coordinated with the movements of the limbs so as to increase the reach of the limbs when these are in the swing phase (e.g., the ipsilateral side of the anterior part of the body is contracting when the contralateral anterior limb is in the air), which therefore leads to an optimized speed of locomotion.

Similarly to swimming, the speed of trotting can be modulated by varying the frequency of oscillation through the level of tonic input applied to both the body and the limb CPGs (Fig. 9). Maximum speed is reached when the frequency of oscillation is around 4.0 Hz. Above 4.0 Hz, the speed does not increase because the increase of frequency (and of amplitude of motoneuron oscillations) is counterbalanced by a reduction in the amplitude of limb and body movements. In this mechanical simulation, the frequency limit above

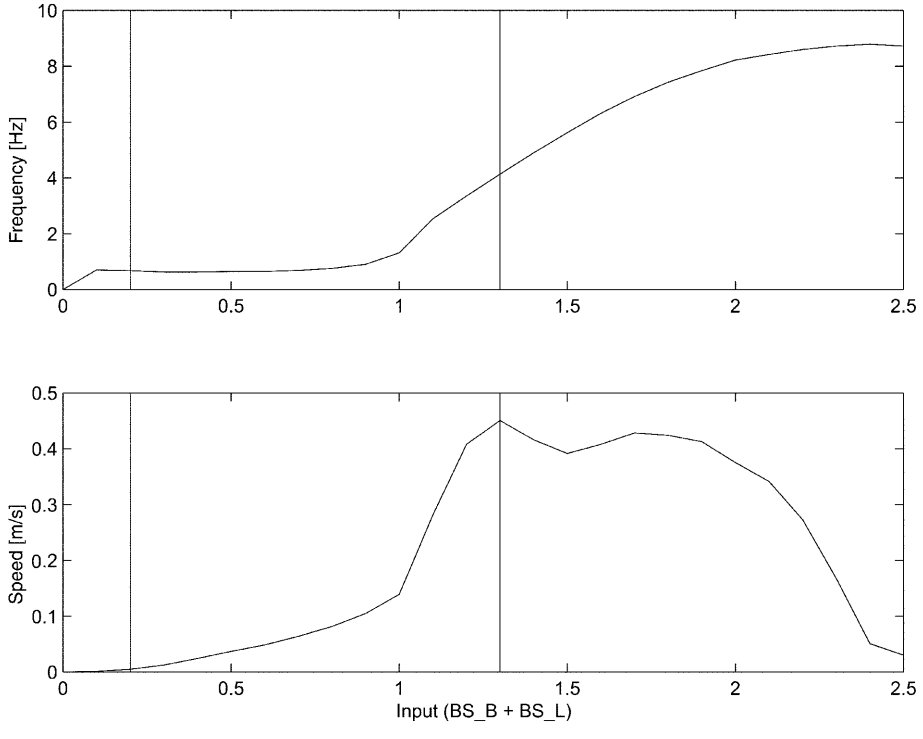

Fig. 9. Complete CPG: influence of the tonic input on the frequency of oscillation and the speed of trotting. The vertical lines determine the region in which the speed increases monotonically with the tonic input (speeds varying from 0.0 to 0.45 m/s when the input varies from 0.2 to 1.3)

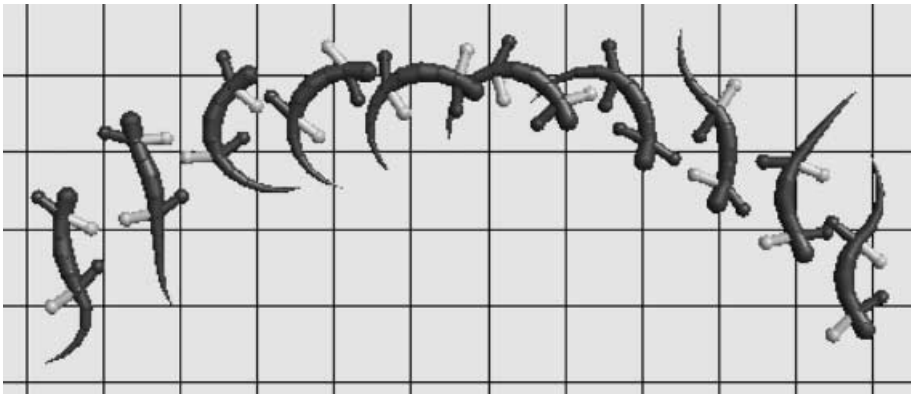

Fig. 10. Turning during trotting induced by asymmetric tonic input

which the speed of locomotion ceases to increase with the frequency is therefore lower for the trotting gait than for the swimming gait. Such a mechanical limitation to the maximum speed during terrestrial locomotion might explain the lower trotting frequencies compared to the swimming frequencies observed in real salamanders (Frolich and Biewener 1992; Delvolvé et al. 1997) – Frolich and Biewener (1992) report, for instance, trotting frequencies from 0.6 to 2.0 Hz, and swimming frequencies from 2.0 to 4.0 Hz in *Ambystoma Tigrinum*.

Turning can be induced by applying asymmetrical input between left and right (Fig. 10). We tested three different cases, applying asymmetry input: (1) to the body CPG, (2) to the limb CPG, and (3) to both the body and limb CPGs. We found that applying asymmetry to only the limb CPG has little effect on the direction of motion, and that the most efficient turning is obtained when the asymmetry is given to the body CPG, or both the body CPG and the limb CPG. The asymmetry of input to the body CPG leads to extra bendings towards the side receiving more excitation, enabling therefore relatively sharp changes of direction.

The complete controller can produce smooth transitions between trotting and swimming gaits. Figure 11 shows the neural activity in the limb and body CPGs during a trot-swim-trot sequence. The sequence is obtained by giving a constant tonic drive of 1.3 to the body CPG, and a sequence of 1.3, −1.5, 1.3 tonic drive to the limb CPG. The limb CPG is therefore turned on-off-on, which means that it switches between forcing the body CPG to produce a standing wave and releasing it to produce the traveling wave. As the limb CPG produces slow oscillations when it receives no tonic drive, it has to be actively inhibited (the −1.5 signal) in order to silence all its interneurons (note that the oscillators could be easily modified to be silent without external excitation, by decreasing the biases of their neurons). During swimming, a tonic drive of 2.0 is given to the limb retractor motoneurons, in order to keep the limbs against the body. After the swimming gait, the trotting gait resumes after a short delay. The delay is due to the time needed for the limb CPG to pass from the almost symmetrical state – forced by the temporary inhibition – to the asymmetrical trotting gait. This sequence is therefore an illustration of the stability of the pattern generation of the locomotor controller.

5 Discussion

5.1 Modeling approach

This article describes the design of a potential control mechanism underlying the aquatic and terrestrial gaits of the salamander. The locomotor circuit is implemented as a leaky-integrator neural network, i.e., it is composed of abstract neuron models which are simpler than detailed compartmental models of neurons but which still encapsulate essential characteristics of neurons such as a nonlinear time-delayed response to synaptic inputs. These types of neurons are particularly suited to the investigation of the dynamics of whole networks because they do not require the setting of too many parameters – if more detailed compartmental models of neurons had been used, their higher modeling accuracy would have been lost in the higher uncertainty of realistically determining their multiple parameters. Futhermore, they are not too computationally expensive, which makes the simulation of a whole network embedded into a mechanical simulation tractable.

Although leaky-integrator neurons are relatively simple, designing a network composed of several hundreds of neurons (344 in this case) requires the setting of many parameters. The real-number genetic algorithm proved to be a useful tool for determining those parameters, given a high-level description of the desired outputs of the network. Techniques from artificial neural networks and artificial intelligence can indeed bring a useful contribution to computational neuroscience by automatizing part of the modeling process. Recent examples include the use of back-propagation algorithms for determining the synaptic weights of locomotor circuits in leech (Lockery and Sejnowski 1997) and in stick insect (Cruse et al. 1995). Similarly, evolutionary algorithms (Holland 1975; Schwefel 1995; Michalewicz 1996) are increasingly used with neural networks, for example when developing neural locomotion controllers for hexapod locomotion (Beer and Gallagher 1992; Gruau 1995; Kodjabachian and Meyer 1998), for setting parameters of compartmental models of single neurons

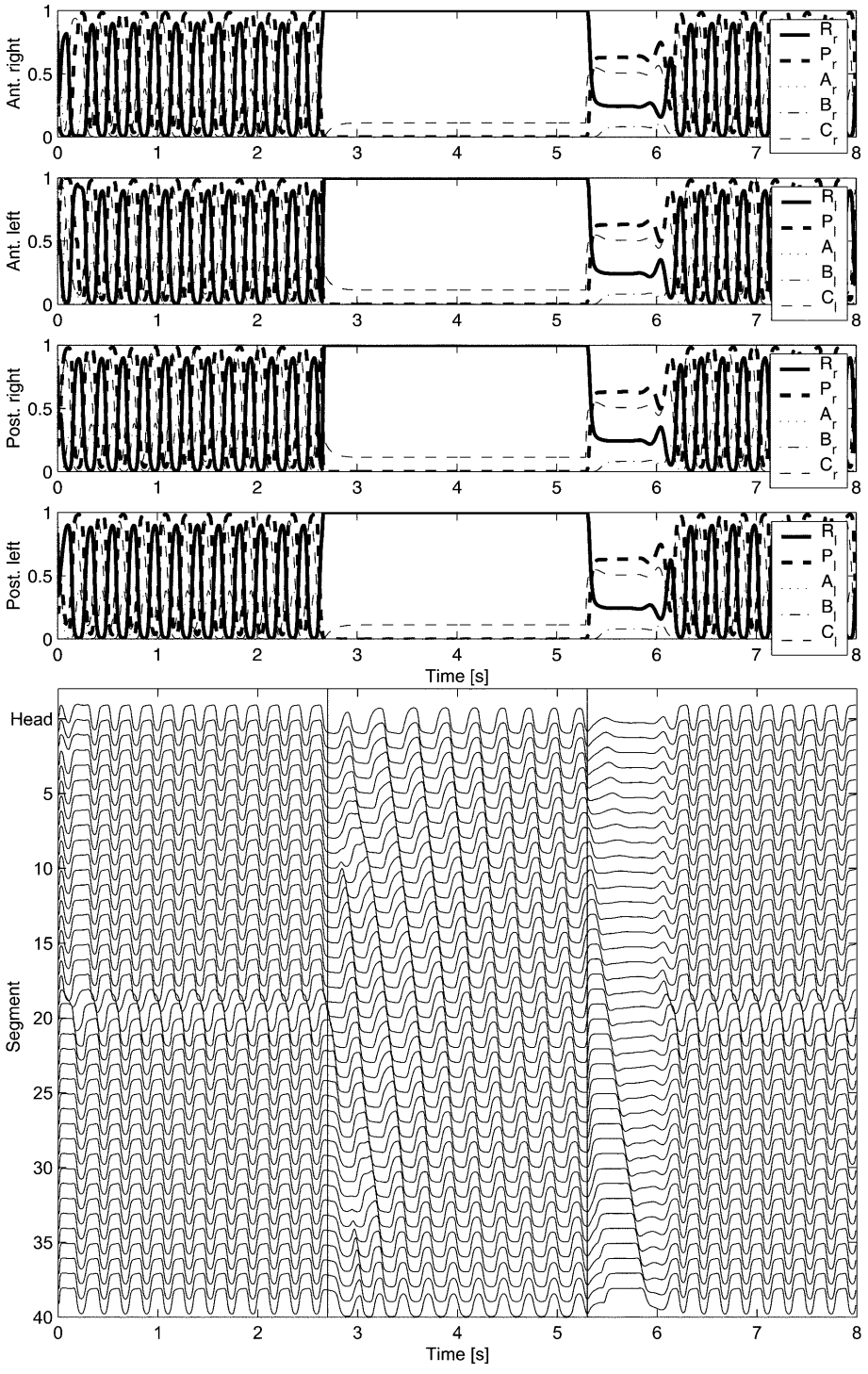

Fig. 11. Gait transition. The body CPG (*bottom*) receives a constant tonic input of 1.3, while the limb CPG (*top*) receives a 1.3 signal from time 0.0 s to 2.7 s, a −1.5 signal from time 2.7 s to 5.3 s, and a 1.3 signal from time 5.3 s to 8.0 s (see text)

(West and Wilcox 1997), or for defining synaptic weights in a model of the salamander's visual system (Eurich et al. 1995). In Ijspeert et al. (1999), we used a similar approach as the one presented here to automatically generate part of Ekeberg's model of the swimming circuit of the lamprey (Ekeberg 1993). We found that the genetic algorithm could successfully generate set of synaptic weights for that circuit, and optimize Ekeberg's hand coded model in terms of the range of frequencies the circuit could produce. On a related note, Ijspeert and Kodjabachian (1999) describes how swimming circuits for the lamprey can be generated in a single evolutionary stage using a more sophisticated genetic encoding scheme in which developmental rules rather than network parameters are evolved.

Evolutionary algorithms (EAs) present several interesting features for the design of connectionist models compared to supervised learning algorithms that are traditionally used in artificial neural networks. Supervised learning algorithms such as variations of the backpropagation algorithm (see for instance, Pearlmutter 1995) iteratively update synaptic weights given

the gradient of an error function which calculates the difference between the current and the desired state-space trajectories of the network (limit cycles, in our case). These algorithms are therefore restricted to problems in which the desired state trajectory is known in advance, which is not the case for many control problems, especially if the plant to be controlled has its own complex nonlinear dynamics (such as a musculoskeletal system, for instance). Those types of problems are better tackled using a reinforcement learning approach (see, e.g., Barto 1995), in which the structure of the network is updated based on a reinforcement signal after a complete control sequence. EAs can be considered an extreme case of reinforcement learning in which the reinforcement signal (the fitness value) is optimized by the evolution of a whole population of potential solutions, and in which the reinforcement signal can potentially be based on multiple control sequences. As such, EAs have several interesting characteristics with the only drawback being that they are computationally expensive. First, the fitness function does not need to be differentiable or even continuous. Second, using an EA allows us to characterize the desired behavior of the network at a "high" level, for instance in terms of the range of frequencies which can be produced or in terms of the speed of locomotion of the mechanical simulation. And finally, the parallel and stochastic nature of EAs makes them less likely to be trapped in a local optimum than other (e.g., gradient-descent) algorithms.

5.2 Salamander locomotion

The locomotor circuit developed in this article is capable of producing the typical swimming and trotting gaits of the salamander. As the locomotor circuit in the salamander has not been decoded for the moment, the proposed circuitry is only hypothetical. Its organization is however based on the hypothesis presented in (Cohen 1988) (see also Delvolvé et al. 1997) that the salamander's locomotor circuit is an extension of lamprey-like swimming circuitry. The argument is that during evolution from a lamprey-like ancestor, the coevolution of bodies and locomotor circuits has seen the generation of fins and then limbs accompanied by a specialization of some segmental oscillators to control these new limbs. As the salamander has kept a partially aquatic habitat, it has kept the control circuitry for aquatic locomotion and has developed a new motor program for terrestrial locomotion. In our model, we assume that the gait transition between swimming and trotting is obtained by the modulation of simple non-oscillating signals from the brainstem.

The body CPG developed is, similarly to the lamprey, a chain of segmental oscillators that propagates a rostrocaudal traveling wave. There are still diverging views on the origin of these phase lags in the lamprey, in particular whether they are due to differences in the intrinsic frequencies of the oscillators or to the nature of the coupling and, in the latter case, whether the dominant coupling is ascending or descending (see for instance Matsushima and Grillner 1992; Williams and Sigvardt 1994; Kopell 1995; Wadden et al. 1997; Hellgren et al. 1999). The argument in favor of a difference in intrinsic frequencies comes from the observation that the lamprey is capable of producing traveling waves with different wavelengths, and even waves which travel backward (i.e. caudorostrally) (Matsushima and Grillner 1992; Grillner et al. 1995). These data tend to show that the lamprey has a mechanism for actively changing the intrinsic frequencies of some segmental oscillators along the spinal cord (for instance by giving more or less tonic input to segments at the extremities). The argument in favor of the intersegmental coupling as the origin of the traveling waves comes from the observations that spinal preparations of the lamprey tend to propagate a rostrocaudal wave during uniform excitatory bathes, while no systematic (passive) differences of intrinsic frequencies have been measured in subparts of the spinal cord (Williams et al. 1990). Predictions from mathematical models of chains of nonlinear oscillators (see Williams and Sigvardt 1994; Sigvardt and Williams 1996) tend to favor this view.

In our opinion, the two hypotheses are not contradictory. One could imagine having circuitry that favors rostrocaudal waves but in which the exact wavelength of the motion can be modulated by giving more or less excitation to the segments at the extremities. Ekeberg's model (Ekeberg 1993), for instance, is based on these two principles and is capable of reproducing most of the observations above. Although Ekeberg's model does not spontaneously produce traveling waves with a constant level of tonic input (it requires some extra excitation on the most rostral segments), it can be modified to do so (Ijspeert et al. 1999).

In this article we describe a body CPG which, when tonic input is applied to it, spontaneously propagates a traveling wave without requiring a difference in the intrinsic frequencies along the spinal cord. The wavelength corresponds then to the length of the body, but it can be modified (reduced) when extra excitation is given to the most rostral segments. The spontaneous wave propagation is in agreement with the recent observations of fictive swimming patterns induced by excitatory bathes in spinal preparations of newts (Delvolvé et al. 1999). Note that in Delvolvé et al. (1999), two types of neural activities were observed, one corresponding to "fast" rostrocaudal waves, the other to much slower caudorostral waves. These caudorostral waves may however be due to the non-uniform sensitivity of segments to the excitatory bath, with segments at the sectioned caudal extremity being more sensitive and therefore more excited (J.M. Cabelguen, personal communication).

Neural waves with a wavelength corresponding to approximately the length of the body have also been measured by EMG recordings during swimming in salamander (Frolich and Biewener 1992) and newt (Delvolvé et al. 1999). In (Frolich and Biewener 1992), the phase lag is observed to be almost constant along the spinal cord, while in Delvolvé et al. (1999), where recordings have been made in more segments, there appears to be three – instead of one – traveling waves

with slightly different phase lags (one in the neck, one in the trunk, and one in the tail). The authors suggest that the difference in phase lags could be due to a tonic influence of the limb CPG on two body segments during swimming.

One of our main aims was to investigate which type of neural mechanism can produce and switch between traveling and standing neural waves. These two types of waves have very distinct phase relations, and it remains a puzzle as to which mechanism is active in the salamander for producing them. In Ermentrout and Kopell (1994), the production of S-shaped standing waves was mathematically investigated in a chain of coupled nonlinear oscillators with long-range couplings. In that model, the oscillators are coupled with closest-neighbor couplings, which tend to make oscillators oscillate in synchrony, and with long-range couplings between oscillators 1 and $m+1$ and between oscillators m and $2m$ in a $2m$-long chain, which tend to make these coupled oscillators oscillate in anti-phase. It is found that for a range of strengths of the long range inhibitory coupling, a S-shaped standing wave is a stable solution. Traveling waves can also be obtained, but only by changing the parameters of the coupling. The biological plausibility of the system as a model of gait transition is therefore limited.

In this article, a neural mechanism of gait transition is proposed which relies on the modulation of an input signal, rather than a rewiring of the circuit. Similar approaches have been taken to model gait transition (e.g. from walk to trot to gallop) in mammals (Collins and Richmond 1994; Canavier et al. 1997), based on observations of gait transition stimulated by simple electric signals in cats (for instance Shik et al. 1966; Grillner et al. 1988). The proposed locomotor circuit is composed of a limb CPG that is coupled unilaterally to a body CPG. The body and the limb CPGs can be stimulated independently by tonic signals from the brainstem. Our model is therefore similar to the neural mechanism suggested in Delvolvé et al. (1997), with the main difference being in the coupling from the limb oscillators to the body segments (in their model, the posterior oscillator projects to some segments in the trunk, and not to the tail segments except for the most caudal). Simulations show that, when modulated by different signals from the brainstem, our proposed locomotor circuit is capable of producing the two distinct motor programs measured by EMG recordings during swimming and trotting (Frolich and Biewener 1992; Delvolvé et al. 1997). The pattern generation is robust and allows for a smooth transitions between swimming and trotting, as well as for modulation of the speed and direction of motion. Anatomical and physiological studies could test the validity of the model by investigating whether two distinct limb oscillatory circuits exist, and whether these circuits project through relatively long-range projections to each other and to body segments. It is also important to investigate whether there are separate pathways for efferent signals from the brainstem.

The mechanical simulation allowed us to investigate how neural activity could modulate gaits in a simple body. Although the biomechanical simulation is only a first approximation to a real salamander, several interesting observations have been made. Realistic swimming and trotting motions are produced, with traveling undulations of the body propelling the body forward in water, and stepping movements pushing the body forward on ground. In the third evolutionary stage, it is interesting to see that a fitness function which optimized the speed of locomotion led to a body-limb coordination very similar to that observed in the salamander. Speed is then optimized because body and limb movements are coordinated so as to increase the reach of the limbs when they are in the swing phase. Finally, the mechanical simulation allowed us to demonstrate the capacity of the locomotor circuit to modulate the speed and direction of motion when its tonic input is varied.

Current work investigates how proprioceptive sensory feedback can be integrated by the locomotor circuit, for shaping the neural activity and ensuring it remains coordinated with the actual movements of the body and limbs during perturbations. We are also extending the neuromechanical model to represent and control a three-dimensional salamander's body with more realistic limbs.

6 Conclusion

This article described the development of a neuromechanical model of salamander locomotion. Using a genetic algorithm, a locomotor circuit was developed that is capable of producing the salamander's typical swimming and trotting gaits in a biomechanical simulation. In particular, a neural mechanism is proposed for the production of both traveling and standing neural waves. The locomotor circuit is based on a lamprey-like body CPG extended by limb oscillators. Smooth gait transition is obtained by varying how tonic input is applied to the circuit. Modulation of tonic input also enables modulation of the speed and direction of motion of the simulated salamander.

Appendix A: Mechanical simulation

The mechanical simulation of the salamander is an extension of the lamprey model developed by Ekeberg (Ekeberg 1993).

A.1 Geometry of the body

The ten-link body is 25 cm long. Each link is 2.5 cm long and has an elliptical cross section of 2.5 cm height and a width that depends on its position along the spinal cord (see Table A1). The legs are cylinders of 4 cm length and 1.5 cm width. They are attached by one degree of freedom joints to the second and the sixth links of the body (Fig. 1). The density of the salamander is assumed to be constant and equal to that of water (1000 Kg/m^3).

Table A1. Parameters for the mechanical simulation. Links 1 to 10 are the body links, links 11 to 14 are the limb links (see Fig. 1). Forelimbs and hindlimbs are identical

Link i	w_i (mm)	m_i (g)	I_i (g mm^2)	$\lambda_{i,\perp}$ (Ns^2/m^2)	$\lambda_{i,\parallel}$ (Ns^2/m^2)
1	23	11.3	961	0.31	0.3
2	22	10.8	889	0.31	0.2
3	25	12.3	1119	0.31	0.1
4	28	13.7	1389	0.31	0.0
5	22	10.8	889	0.31	0.0
6	18.6	9.1	674	0.31	0.0
7	15.2	7.4	498	0.31	0.0
8	11.8	5.8	354	0.31	0.0
9	8.5	4.2	235	0.31	0.0
10	5.1	2.5	134	0.31	0.0
11–14	15	7.1	1042	0.30	0.1

A.2 Newton's laws of motion

The laws of motion are solved in the horizontal plane. x_i and y_i give the position of the center of the link i and φ_i is its angle. The acceleration of each link i depends on: $\vec{\mathbf{E}}_i$, the forces exerted by the environment; on O_i, the torques due to body-limb contacts; on G_i, the torques due to limb-ground contacts; on T_i^j, the torques due to the paired muscles of joint(s) j; and on $\vec{\mathbf{C}}_i^j$, the inner forces due to the constraints of joint(s) j:

$$m_i\ddot{x}_i = E_{i,x} + \sum_j C_{i,x}^j \tag{3}$$

$$m_i\ddot{y}_i = E_{i,y} + \sum_j C_{i,y}^j \tag{4}$$

$$I_i\ddot{\varphi}_i = \sum_j T_i^j + O_i + G_i - \sum_j C_{i,x}^j \frac{l_i}{2}\sin\varphi_i + \sum_j C_{i,y}^j \frac{l_i}{2}\cos\varphi_i \tag{5}$$

where m_i and I_i are the mass and the moment of inertia of link i and l_i is the length of the link. Leg links and links at the extremities of the body (links 1 and 10) have only one joint (and muscle torque). Body links 3, 4, 5, 7, 8, and 9 have two joints (body links are counted from the head to the tail, i.e., link 1 is the head link). Links 2 and 6 have four joints (and muscle torques), i.e., those corresponding to the chain of body links and those of the opposite legs. Table A1 gives the masses and moments of inertia of the different links.

A.3 Inner forces

The inner forces $\vec{\mathbf{C}}_i^j$ ensure that links of the articulated body stay connected. These forces are calculated explicitly based on the computation of the Jacobian of the function representing the geometrical constraints induced by each joint (for details see Ekeberg 1993). Similarly to Ekeberg (1993), attached links are prevented from drifting apart with the accumulation of numerical errors by using the *stabilization through projection* technique, which periodically adjusts the system to conform to the constraints. Unlike Ekeberg (1993), the stabilization is applied only when the error in the joints exceeds a given threshold, rather than for every tenth integration step.

A.4 Muscle torques

A muscle is simulated as a combination of spring and damper. The torques exerted on each joint are determined by a pair of antagonist extensor and flexor muscles (i.e., the left-right muscles of the body and the retractor and protractor muscles of the limbs). These muscles can be contracted by input signals from motoneurons, which increase their spring constant and therefore reduce their resting length. The torque acting at a particular joint is therefore determined by the motoneuron activities (M_e and M_f) of the antagonist flexor and extensor muscles:

$$T = \alpha(M_f - M_e) + \beta(M_f + M_e + \gamma)\Delta\varphi + \delta\Delta\dot{\varphi} \tag{6}$$

where $\Delta\varphi$ is the difference between the actual angle of the joint and the resting angle. The coefficients α, β, γ, and δ determine, respectively, the gain, the stiffness gain, the tonic stiffness, and the damping coefficient of the muscles. These values vary slightly depending on the type of joint (Table A2). They have been set by hand so that the resulting torques are sufficient to move the 116 g weight of the 25-cm long body at swimming and trotting speeds that correspond approximately to real salamanders of the same size (for instance see Frolich and Biewener 1992).

A.5 Body-limb contact torques

These torques prevent the limbs from penetrating into the body. Once there is a contact between a cylinder representing a body link and the extremity of the cylinder representing a limb i (i = 11,...,14), an elastic and damping torque is computed and applied to the limb: $O_i = -a\theta - b\dot{\theta}$, where θ is the angle corresponding to how much the limb penetrates into the body link, $a = 1250$ N mm is an elasticity constant, and $b = 25\,000$ N mm ms is a damping constant. For simplification, the contact-related forces and torques acting on the body link are not computed.

Table A2. Muscle parameters

	α (N mm)	β (N mm)	γ	δ (N mm ms)
Body joint	15	1.5	10.0	200
Leg joint	20	2.0	6.0	200

A.6 Forces due to the environment: in water

Similarly to Ekeberg (1993), it is assumed that the speed of the water relative to the body is sufficiently high for the forces exerted by the water to be mainly inertial (i.e., high Reynolds number). It is also assumed that the water is stationary and that the parallel and perpendicular components of the force exerted by the water on each link can be calculated separately. These components of the force on each link ($i = 1,\ldots,14$) can therefore be calculated as:

$$E_{i,\parallel} = \lambda_{i,\parallel} v_{i,\parallel}^2 \tag{7}$$

$$E_{i,\perp} = \lambda_{i,\perp} v_{i,\perp}^2 \tag{8}$$

where

$$\lambda_{i,\parallel} = \tfrac{1}{2} C_{i,\parallel} S_i \rho \tag{9}$$

$$\lambda_{i,\perp} = \tfrac{1}{2} C_{i,\perp} S_i \rho \tag{10}$$

$v_{i,\parallel}$ and $v_{i,\perp}$ are the components of the velocity of the link i relative to the water. $\lambda_{i,\parallel}$ and $\lambda_{i,\perp}$ are coefficients that depend on the density of the fluid ρ, the area perpendicular to the movement S_i, and the drag coefficients $C_{i,\perp}$ and $C_{i,\parallel}$ that are dependent on the shape of link i (here $C_{i,\perp} = 1$ for all links, and $C_{i,\parallel} = 0$ for all links except the limbs and the three trunk links closest to the head; see Table A1). Note that these hydrodynamic forces are only first approximations to the forces involved in fluid-body interactions. For a more detailed numerical study of the hydrodynamics of anguiliform swimming, see Carling et al. (1998).

A.7 Forces due to the environment: on ground

On ground, all trunk and tail links are subjected to a dynamic friction force, since the body of the salamander slides on the ground when the salamander is trotting. The friction force on trunk-tail link i ($i = 1, \ldots, 10$) is:

$$\vec{\mathbf{E}}_i = \begin{cases} \vec{\mathbf{0}} & \text{when } \vec{\mathbf{v}}_i = (\dot{x}_i, \dot{y}_i) = (0,0) \\ -\mu g m_i \frac{\vec{\mathbf{v}}_i}{||\vec{\mathbf{v}}_i||} & \text{otherwise} \end{cases} \tag{11}$$

where $\vec{\mathbf{v}}_i$ is the velocity of link i, g is the gravity constant ($9.81\,\mathrm{m/s^2}$), and μ the friction constant which was set to 0.3.

As only the accelerations in the horizontal plane are considered, vertical movements of the limbs are not calculated, and instead the position of the extremity of the limb (the foot), in the air or on the ground, is assumed to be determined by the signals sent to the limb muscles. The limb i ($i = 11, \ldots, 14$) is assumed to be in the air ($\vec{\mathbf{E}}_i = \vec{\mathbf{0}}$ and $G_i = 0$) when the signal of the protractor is larger than that of the retractor, and on the ground otherwise. The contact of a limb with the ground is then represented as a dynamic friction force $\vec{\mathbf{E}}_{\text{foot}}$ applied to the extremity of the limb link and opposite to the motion of that point:

$$\vec{\mathbf{E}}_{\text{foot}} = \begin{cases} \vec{\mathbf{0}} & \text{when } \vec{\mathbf{v}}_{\text{foot}} = \vec{\mathbf{0}} \\ -\eta \frac{\vec{\mathbf{v}}_{\text{foot}}}{||\vec{\mathbf{v}}_{\text{foot}}||} & \text{otherwise} \end{cases} \tag{12}$$

where $\vec{\mathbf{v}}_{\text{foot}}$ is the velocity of the foot (the contact point) and η is a constant equal to 0.5N. This friction force on the foot leads to the following force $\vec{\mathbf{E}}_\mathbf{i}$ and torque G_i on the corresponding limb link i:

$$\vec{\mathbf{E}}_i = \vec{\mathbf{E}}_{\text{foot}} \tag{13}$$

$$G_i = -\frac{l_i}{2} \sin\varphi_i \, E_{\text{foot},x} + \frac{l_i}{2} \cos\varphi_i \, E_{\text{foot},y} \tag{14}$$

Note that when two opposing limbs are on the ground at the same time, the motion of the salamander is braked by the friction forces applied to the extremities of both limbs.

Acknowledgements. I gratefully acknowledge Michael Arbib and Stefan Schaal for their constructive comments on this project. Special thanks to Jean-Marie Cabelguen for his insightful comments on an earlier version of this paper. Thanks also to an anonymous reviewer for useful remarks. Facilities were provided by the University of Southern California. This work was supported by a researcher grant from the Swiss National Science Foundation.

References

Barto A (1995) Reinforcement learning in motor control. In: Arbib M (ed) The handbook of brain theory and neural networks. MIT Press, Cambridge, Mass., pp 809–813

Beer R (1995) On the dynamics of small continuous-time recurrent neural networks. Adapt Behav 3: 469–510

Beer R, Gallagher J (1992) Evolving dynamical neural networks for adaptive behavior. Adapt Behav 1: 91–122

Beer R, Chiel H, Quinn R, Espenshied K, Larsson P (1992) A distributed neural network architecture for hexapod robot locomotion. Neural Comput 4: 356–365

Cacciatore T, Rozenshteyn R, Kristan W (2000) Kinematics and modeling of leech crawling: evidence for an oscillatory behavior produced by propagating waves of excitation. J Neurosci 20: 1643–1655

Canavier C, Butera R, Dror R, Baxter D, Clark J, Byrne J (1997) Phase response characteristics of model neurons determine which patterns are expressed in a ring circuit model of gait generation. Biol Cybern 77: 367–380

Carling J, Williams T, Bowtell G (1998) Self-propelled anguiliform swimming: simultaneous solution of the two dimensional Navier-Stokes equations and Newton's laws of motion. J Exp Biol 201: 3143–3166

Cohen A (1988) Evolution of the vertebrate central pattern generator for locomotion. In: Cohen AH, Rossignol S, Grillner S (eds) Neural control of rhythmic movements in vertebrates. John Wiley and Sons, New York

Collins J, Richmond SA (1994) Hard-wired central pattern generators for quadrupedal locomotion. Biol Cybern 71: 375–385

Cruse H, Brunn D, Bartling C, Dean J, Dreifert M, Kindermann T, Schmitz J (1995) Walking: A complex behavior controlled by simple networks. Adapt Behav 3: 385–418

Delvolvé I, Bem T, Cabelguen JM (1997) Epaxial and limb muscle activity during swimming and terrestrial stepping in the adult newt, *Pleurodeles waltl*. J Neurophysiol 78: 638–650

Delvolvé I, Branchereau P, Dubuc R, Cabelguen J-M (1999) Fictive rhythmic motor patterns induced by NMDA in an in vitro

brain stem–spinal cord preparation from an adult urodele. J Neurophysiol 82: 1074–1077
Ekeberg Ö (1993) A combined neuronal and mechanical model of fish swimming. Biol Cybern 69: 363–374
Ekeberg Ö, Wallén P, Lansner A, Traven H, Brodin L, Grillner S (1991) A computer based model for realistic simulations of neural networks. I. The single neuron and synaptic interaction. Biol Cybern 65: 81–90
Ekeberg Ö, Lansner A, Grillner S (1995) The neural control of fish swimming studied through numerical simulations. Adapt Behav 3: 363–384
Ermentrout B, Kopell N (1994) Learning of phase lags in coupled neural oscillators. Neural Comput 6: 225–241
Eurich W, Roth G, Schwegler H, Wiggers W (1995) Simulander: a neural network model for the orientation movement of salamanders. J comp physiol 176: 379–389
Frolich L, Biewener A (1992) Kinematic and electromyographic analysis of the functional role of the body axis during terrestrial and aquatic locomotion in the salamander *Ambystoma tigrinum*. J Exp Biol 62: 107–130
Getting P (1989) Reconstruction of small neural networks. In: Koch C, Segev I (eds) Methods in neural modeling, MIT Press, Cambridge, Mass., pp 171–196
Goldberg DE (1989) Genetic Algorithms in Search, Optimization, and Machine Learning. Addison-Wesley, Reading, Mass
Grillner S, Buchanan J, Wallén P, Brodin L (1988) Neural control of locomotion in lower vertebrates. In: Cohen AH, Rossignol S, Grillner S (eds) Neural control of rhythmic movements in vertebrates. John Wiley and Sons, New York, pp 1–40
Grillner S, Wallén P, Brodin L (1991) Neuronal network generating locomotor behavior in lamprey: Circuitry, transmitters, membrane properties, and simulation. Ann Rev Neurosci 14: 169–199
Grillner S, Degliana T, Ekeberg Ö, El Marina A, Lansner A, Orlovsky G, Wallén P (1995) Neural networks that co-ordinate locomotion and body orientation in lamprey. Trends Neurosci 18: 270–279
Gruau F (1995) Automatic definition of modular neural networks. Adapt Behav 3: 151–184
Hellgren J, Grillner S, Lansner A (1992) Computer simulation of the segmental neural network generating locomotion in lamprey by using populations of network interneurons. Biol Cybern 68: 1–13
Hellgren J, Kotaleski J, Grillner, S, Lansner A (1999) Neural mechanisms potentially contributing to the intersegmental phase lag in lamprey. I. Segmental oscillations dependent on reciprocal inhibition. Biol Cybern 81: 317–330
Holland J (1975) Adaptation in natural and artificial systems. University of Michigan Press, ANN ARBOR
Hopfield J (1984) Neurons with graded response properties have collective computational properties like those of two-state neurons. Proc Nat Acad Sci USA 81: 3088–3092
Ijspeert A, Kodjabachian J (1999) Evolution and development of a central pattern generator for the swimming of a lamprey. Artif Life 5: 247–269
Ijspeert A, Hallam J, Willshaw D (1999) Evolving swimming controllers for a simulated lamprey with inspiration from neurobiology. Adap Behav 7: 151–172
Kimura H, Akiyama S, Sakurama K (1999) Realization of dynamic walking and running of the quadruped using neural oscillators. Autonomous Robots 7: 247–258
Kodjabachian J, Meyer J-A (1998) Evolution and development of neural networks controlling locomotion, gradient-following, and obstacle-avoidance in artificial insects. IEEE Trans Neural Netw 9: 796–812
Kopell N (1995) Chains of coupled oscillators. In: Arbib M (ed) The handbook of brain theory and neural networks. MIT Press, Cambridge, Mass., pp 178–183
Lockery S, Sejnowski T (1993a) The computational leech. Trends Neurosci 16: 283–290
Lockery S, Sejnowski T (1993b) Voyages through weight space: network models of an escape reflex in the leech. In: Beer R, Ritzman R, McKenna T (eds) Biological neural networks in invertebrated neuroethology and robotics. Academic, Boston
Matsushima T, Grillner S (1992) Neural mechanisms of intersegmental coordination in lamprey: local excitability changes modify the phase coupling along the spinal cord. J Neurophysiol 67: 373–388
Michalewicz Z (1996) Genetic Algorithms + Data Structures = Evolution programs. Springer, Berlin Heidelberg New York
O'Donovan M, Wenner P, Chub N, Tabak J, Rinzel J (1998) Mechanisms of spontaneous activity in the developing spinal cord and their relevance to locomotion. In: Kiehn O, Harris-Warrick R, Jordan L, Hultborn H, Kudo N (eds) Neuronal Mechanisms for Generating Locomotor Activity. The New York Academy of Sciences, pp 130–141
Pearlmutter B (1995) Gradient calculations for dynamic recurrent neural networks: a survey. IEEE Trans Neural Netw 6: 1212–1228
Roberts A, Tunstall M (1990) Mutual re-excitation with post-inhibitory rebound: A simulation study on the mechanisms for locomotor rhythm generation in the spinal cord of xenopus embryo. Eur J Neurosci 2: 11–23
Schwefel H-P (1995) Evolution and Optimum Seeking. John Wiley, New York
Shik M, Severin F, Orlovsky G (1966) Control of walking by means of electrical stimulation of the mid-brain. Biophy 11: 756–765
Sigvardt K, Williams T (1996) Effects of local oscillator frequency on intersegmental coordination in the lamprey locomotor CPG: theory and experiment. J Neurophysiol 76: 4094–4103
Taga G, Yamaguchi Y, Shimizu H (1991) Self-organized control of bipedal locomotion by neural oscillators in unpredictable environment. Biol Cybern 65: 147–159
Wadden T, Hellgren J, Lansner A, Grillner S (1997) Intersegmental coordination in the lamprey: simulations using a network model without segmental boundaries. Biol Cybern 76: 1–9
Wallén P, Ekeberg Ö, Lansner A, Brodin L, Traven H, Grillner S (1992) A computer-based model for realistic simulations of neural networks. II. The segmental network generating locomotor rhythmicity in the lamprey. J Neurophysiol 68: 1939–1950
West R, Wilcox G (1997) Robust parameter selection for compartmental models of neurons using evolutionary algorithms. In: Bower J (ed) Computational Neuroscience: Trends in Research 1997. Plenum, New York
Williams T (1992) Phase coupling by synaptic spread in chains of coupled neuronal oscillators. Science 258: 662–665
Williams T, Sigvardt K (1994) Intersegmental phase lags in the lamprey spinal cord: experimental confirmation of the existence of a boundary region. J Comput Neurosci 1: 61–67
Williams T, Sigvardt K, Kopell N, Ermentrout G, Rempler M (1990) Forcing of coupled nonlinear oscillators: studies of intersegmental coordination in the lamprey locomotor central pattern generator. J Neurophysiol 64: 862–871